EXPERIMENTAL STUDY OF FLAME SPREAD ON CONVEYOR BELTS IN A SMALL-SCALE TUNNEL

Liming Yuan & Charles D. Litton
National Institute for Occupational Safety and Health
Pittsburgh Research Laboratory
626 Cochrans Mill Road
P.O. Box 18070
Pittsburgh, PA 15236, USA

ABSTRACT

This paper presents experimental results for conveyor belt flame spread from tests conducted in a small-scale tunnel. The purpose of this study is to investigate the effects of belt type, ventilation velocity, belt surface-to-roof distance and ignition source power on the flame spread properties. The tunnel used was 4.9 m long by 0.46 m square with the ventilation velocity ranging from 0.7 to 3.2 m/s. The ignition source was an impinged methane jet burner with heat output ranging from 7 to 21 kW. The belts tested included non-fire resistant rubber belts, fire-resistant rubber belts, fire-resistant neoprene belt and fire-resistant PVC belt with belt samples measuring 0.23 m wide by 2.5 m long. Experimental results show that with a ventilation velocity of 1.02 m/s all conveyor belts could be ignited, and that with sufficient ignition source power, flames spread the full length of the belt sample. The data showed a coupling effect of the ventilation air velocity and the belt surface-to-roof distance on the flame spread rate. For instance, flames could not spread with a ventilation velocity higher than 1.52 m/s and a surface-to-roof distance of 0.22 m. The use of the measured CO/CO_2 ratio as an indicator of combustion stoichiometry is also discussed.

Disclaimer: The findings and conclusions in this report are those of the authors and do not necessarily represent the views of the National Institute for Occupational Safety and Health.

INTRODUCTION

Fires involving conveyor belts continue to be a life threat for U.S. underground miners. From 1990 to 1999, 16 reported fires were caused by conveyor belts in U.S. underground mines causing four injuries [1]. Recently, during the Aracoma Alma mine conveyor belt fire accident in January, 2006, two miners were killed. In order to reduce the fire hazard from conveyor belts, fire-resistant conveyor belts are required in U.S. underground coal mines. The current U.S. flammability test for acceptance of fire-resistant belts for underground coal mines is specified in the Code of Federal Regulations[2] and is conducted by the Department of Labor, Mine Safety and Health Administration (MSHA) Approval and Certification Center. The test is performed in a 0.53 m cubic test chamber using 4 samples 152-mm-long by 12.7-mm-wide by the belt thickness. The sample is positioned horizontally in the chamber, with the transverse axis inclined at 45º, and one end exposed to the flame from a Bunsen type burner for 1 minute in still air. After one minute, the burner flame is removed and the ventilating fan turned on to produce an air current of 1.52 m/s. The duration of the belt flame or glowing is measured. A belt passes the test if four samples of the same belt do not exhibit either duration of flame exceeding an average of 1 minute after removal of the applied flame or afterglow exceeding an average of 3 minutes duration.

A series of large-scale conveyor belt flammability tests were conducted by the former Bureau of Mines [3-5]. The results from these large-scale tests were utilized to develop a new MSHA laboratory-scale test for better evaluating the flame resistance of conveyor belts used in underground coal mines [6, 7]. The schematic of the laboratory-scale test tunnel is shown in Figure 1. The test chamber in the laboratory-

scale tunnel is 1.68 m long by 0.46 m square cross section. The belt sample size is 1.5 m long by 0.23 m wide. The sample is fastened to a steel rack constructed of slotted angle iron with a sample surface to tunnel roof distance of 0.22 m. The igniter is a commercially available 12 impinged jet methane gas burner with a heat output of 21 kW. The duration of gas burner is 5 minutes. The ventilation velocity is set at 1.02 m/s through the tunnel. A belt passes the test if, in three separate trials, there remains a portion of the sample that is undamaged across its entire width. A belt fails the test if in any single trial, fire damage extends to the end of the sample. The results from the laboratory-scale tests were in good agreement with the large-scale tests. In this study, experiments were conducted in a similar laboratory-scale tunnel to investigate the influences of igniter source power, ventilation velocity and belt surface-to-roof distance on the flammability of various conveyor belts.

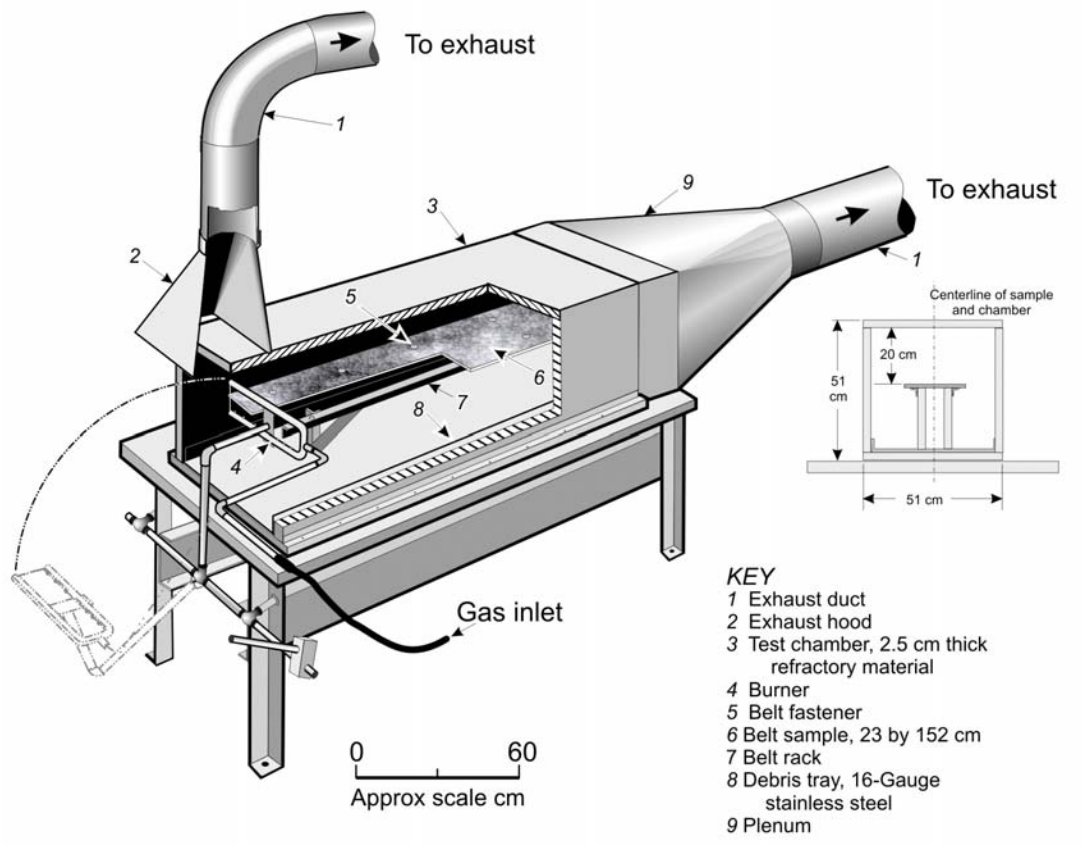

Figure 1. Schematic of laboratory-scale test tunnel [6]

EXPERIMENTAL

Experiments were conducted in a small-scale ventilated tunnel with the same cross section as the one in reference 6 but with a length of 4.9 m. The cross section of the test chamber was 0.46 m x 0.46 m. The chamber was built with 2.5-cm-thick refractory material. At the exhaust end of the 4.9 m tunnel, there was a transition and mixing section where the gases were exhausted to the outside air via a small axivane fan. A sliding damper at the end of the transition and mixing section was used to control the air velocity through the tunnel, and could be varied from 0.0 to 5.1 m/s. The belt sample was 0.23 m wide and 2.5 m long and was mounted on a steel rack constructed of slotted angle iron. Three different heights of racks were used to obtain belt-to-roof distances of 0.34, 0.22, and 0.11 m.

Eight thermocouples were embedded just below the surface of the belt centerline at incremental distances of 0.30 m. The average flame front spread rate along the belt surface was determined from the time-temperature traces obtained from the belt surface thermocouples. A temperature of 310°C was used as the

arrival of the flame front [8]. Thermocouples were also located approximately 0.05 m from the roof at incremental distances of 1.0 m along the tunnel, and a five-thermocouple array located at the exhaust end of the tunnel was used to measure the average gas temperature. A stainless steel gas sampling probe was located in the center of the transition and mixing section which continuously flowed gas samples to the gas analyzers for measurements of CO, CO_2, and O_2. Thermocouple and gas analyzer output signals were sent to a data acquisition system for processing.

Figure 2. The ventilated tunnel with the gas burner igniting a sample belt

The igniter was the same type of commercial 12 impinged jet methane gas burner (two rows of 6 jets) as in reference 6. During each test, a belt sample was fastened with the top cover facing up, if applicable, to the steel rack with 1.4-mm-diameter cotter pins and thin washers to prevent the belt from shrinking away from the burner. The rack was placed in the tunnel and the airflow was set. The airflow was measured by a vane anemometer placed on the belt surface about 30 cm from the front of the tunnel. The methane burner was ignited and the flame was allowed to stabilize. The burner was then applied to the front edge of the belt sample with the flames impinging equally on the top and bottom surfaces of the sample. After 5 minutes, the burner was removed, and the belt sample was allowed to burn until the flames were out. Figure 2 shows the ventilated tunnel with the gas burner igniting a sample belt.

RESULTS AND DISCUSSIONS

Effects of Belt Type and Ignition Source Power

A total of six types of conveyor belts were tested with different ignition source heat output. The belts tested include 2-ply non-fire resistant (NFR) styrene-butadiene (SBR) belt, 3-ply NFR SBR belt, 4-ply NFR SBR belt, 3-ply fire-resistant (FR) SBR belt, FR neoprene belt and FR polyvinyl chloride (PVC) belt. The ventilation air velocity was set at 1.02 m/s. The construction, thickness and heat of combustion of these belts are shown in Table 1. The belt thickness ranged from 9 mm to 15 mm. For the non-fire resistant SBR belts, the values of heat of combustion are very similar for different numbers of plies. The heat of combustion for FR SBR belt is about 20% lower than that for NFR. For FR neoprene and PVC belts, the values are 18.6 and 22.1 kJ/g, respectively.

The test results for the different conveyor belts are shown in Table 2 with three igniter heat outputs of 7 kW, 14 kW and 21 kW, respectively. With the 7 kW ignition heat output, only the NFR SBR conveyor belts with 2 plies and 3 plies could be ignited, and the flame propagated at an averaged velocity of 47

cm/min and 69 cm/min, respectively. For the 4-ply NFR SBR belt and the FR SBR belt, the flame gradually shrunk and died in several minutes after the igniter was turned off. The larger thickness for the 4-ply NFR SBR belt probably hindered the flame spread as the flame spread rate was found to be inversely proportional to the belt thickness for small values of thickness and to approach a constant value as the thickness increases [9]. With the 14 kW ignition heat output, the NFR SBR belts with 2 plies, 3 plies and 4 plies all ignited, and the flame spread at a velocity of 71, 77 and 76 cm/min, respectively, indicating that the flame spread rates were nearly the same for the NFR SBR belts with different plies with the ignition source power of 14 kW. The test results for 2-ply and 3-ply NFR SBR belts also implies that the higher heat output of the burner resulted in the higher flame spread rate for the same kind of belt. FR neoprene and PVC belts still could not be ignited. For the neoprene belt, the flame immediately extinguished after the igniter was turned off, and the belt smoldered heavily. Much smoke was generated from the smoldering belt for a long time. The final charred length was about 0.38 m on the top surface and 0.48 m on the bottom surface. For the PVC belt, the flame extinguished in about 25 seconds after the igniter was turned off. Unlike the neoprene conveyor belt, PVC belt did not smolder very much. The final charred length was about 0.76 m on the top surface and 0.61 m on the bottom surface.

Table 1. Conveyor belt properties

Conveyor Belt	**Construction**	**Thickness (mm)**	**Heat of combustion (kJ/g)**
NFR SBR	2 plies	9	35.4
NFR SBR	3 plies	10	36.1
NFR SBR	4 plies	15	36.8
FR SBR	3 plies	11	28.8
FR Neoprene	Chloroprene solid woven	9	18.6
FR PVC	PVC solid woven	11	22.1

Table 2. Average flame spread rates (m/min)

Conveyor Belt	**Ignition source power (kW)**		
	7	14	21
NFR SBR (2 plies)	0.47	0.71	Not tested
NFR SBR (3 plies)	0.69	0.77	Not tested
NFR SBR (4 plies)	NP	0.76	Not tested
FR SBR (3 plies)	NP	0.30	Not tested
FR Neoprene	Not tested	NP	0.23
FR PVC	Not tested	NP	SF*

NP: no flame propagation; SF*: fast surface flame propagation

With the 21 kW ignition heat output, FR neoprene and PVC belts were both ignited. For the neoprene belt, flame propagated very slowly to the end of the belt at an average velocity of about 23 cm/min. Then, the flame size reduced gradually, and eventually became smoldering. Most of the belt was burned out; only small part of the belt was left and charred. The PVC belt had a fast surface flame propagation on both top and bottom surfaces without burning most of the belt while the igniter was still on. After the igniter was turned off after 5 minutes, the belt continued burning but the flame size reduced gradually for another 10 minutes, then the flame was out. The belt material in the center of the belt was not burned away; the belt was only partially charred on the surface.

Under the conditions studied here, all conveyor belts were ignited and the flames spread with a sufficiently high ignition heat output, 14 to 21 kW, in this study. The difference between NFR belts and FR belts is that FR belts were not ignited with the ignition heat output of 14 kW while NFR belts were ignited and the flames spread at a rate of about 76 cm/min. With the ignition heat output of 21 kW, the neoprene belt had a flame spread rate of 23 cm/min while the PVC belts exhibited a fast surface flame propagation.

Effects of Ventilation Velocity and Belt Surface-to-roof Distance

Figure 3 shows the measured flame front velocities for tests conducted at different ventilation velocities for the FR SBR conveyor belt. Two different belt surface-to-roof distances, 0.11 m and 0.22 m, were used with the igniter heat output of 21 kW. With the belt surface-to-roof distance of 0.11 m, the flame spread rate first increased, then decreased with the increase of ventilation velocity. The flame spread rate peaked at the air velocity of about 2.1 m/s. With the belt surface-to-roof distance of 0.22 m, the flame spread rate decreased with the increase of air velocity, and the flame spread did not occur when the ventilation velocity was greater than 1.52 m/s. Qualitatively, these data agree with data obtained from the large-scale conveyor belt tests [4]. When the air velocity was increased, more oxygen was supplied for the burning of the belt. At the same time, more heat was also carried away by the increased air flow. At a sufficiently high ventilation velocity, the flame could be blown off immediately when the igniter was turned off. But with a lower surface-to-roof distance, the roof would have a higher temperature and would radiate more heat back to the belt surface to maintain the flame spread. This may explain why the flame spread occurred at all imposed air velocities with the surface-to-roof distance of 0.11 m. The air velocity at which the flame spread rate peaked depends not only on the surface-to-roof distance, but also the type of the belt.

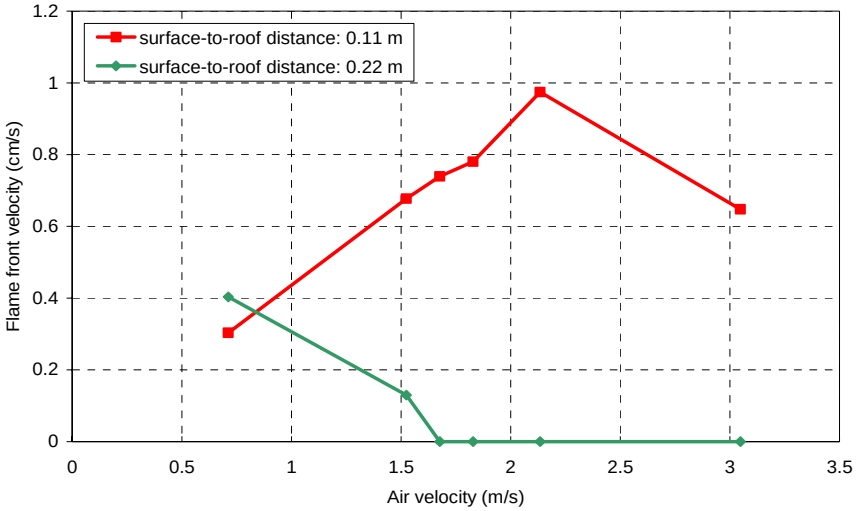

Figure 3. Flame front velocity for the FR SBR belt as a function of the air velocity with the surface-to-roof distance of 0.11 m and 0.22 m

It is worth noting that, for an unconfined, or free-burning belt fire, the flame front velocity increases with the concurrent air velocity, assuming the velocity is not high enough to blow off the flame, as experimentally confirmed by Fernandez-Pello [10]. But in a confined space, like the tunnel in this study, the flame spread rate peaked at a certain air velocity, and then decreased with the further increase of the air velocity. This also happened in the large-scale conveyor belt tests. Figure 4 shows the flame front velocity as a function of the imposed convective air velocity for two types of SBR belts in the large-scale fire gallery tests with a fixed surface-to-roof distance [3, 4]. The measured flame front velocity peaked around the air velocity of 1.5 m/s.

Compared with the burning of combustible materials in open air, the burning of conveyor belts in the tunnel is enhanced because the unburnt portion of the belt downstream is preheated by the convective heat carried by the ventilation flow in addition to the radiative heat from the flame. Close to the flame, the radiation from the flame dominates the heat transfer to the belt surface [11]. The preheating of the belt helps the flame spread as found by Kuchta et al [12]. Figure 5 shows the belt surface temperature history 2.44 m from the leading edge of the belt for six types of conveyor belts with an igniter heat output of 14 kW in the small-scale tunnel. The temperatures at this point immediately after the igniter was turned off for the

conveyor belts are shown in Table 3. Unlike the free-burning, the downstream portion of the belt was significantly heated by the convective heat carried by the air flow before the flame front reached this portion of the belt, especially for three NFR SBR belts, resulting in the fast flame spread rates. For the FR SBR belt, even though the temperature at 2.44-m position at 5 minutes was lower than those for the FR neoprene and PVC belts, the flame still spread slowly, probably because of its higher value of heat of combustion which resulted in more heat release. The estimated heat release rate using measured gas data [13] at 5 minutes was 118, 66.9 and 110 kW for FR SBR, FR neoprene and FR PVC belt, respectively.

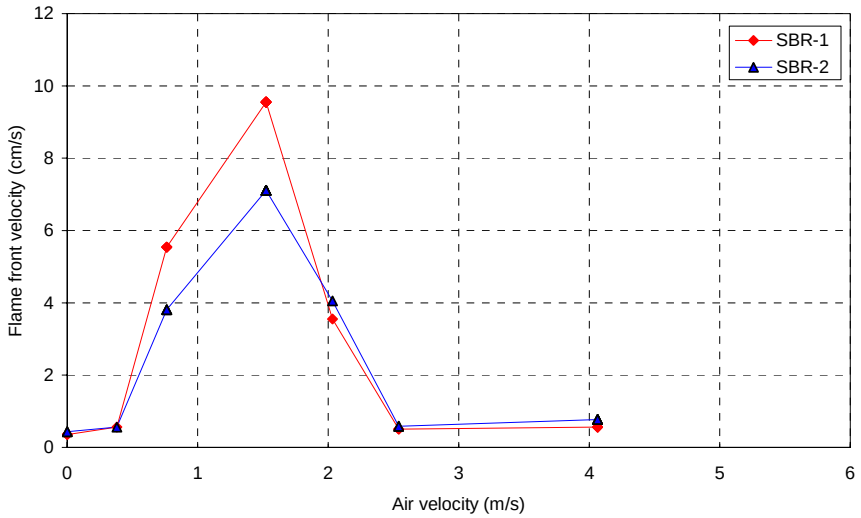

Figure 4. Flame front velocity for two SBR belts in the large-scale experiments as a function of the forced air velocity [4] with the surface-to-roof distance of 1.3 m

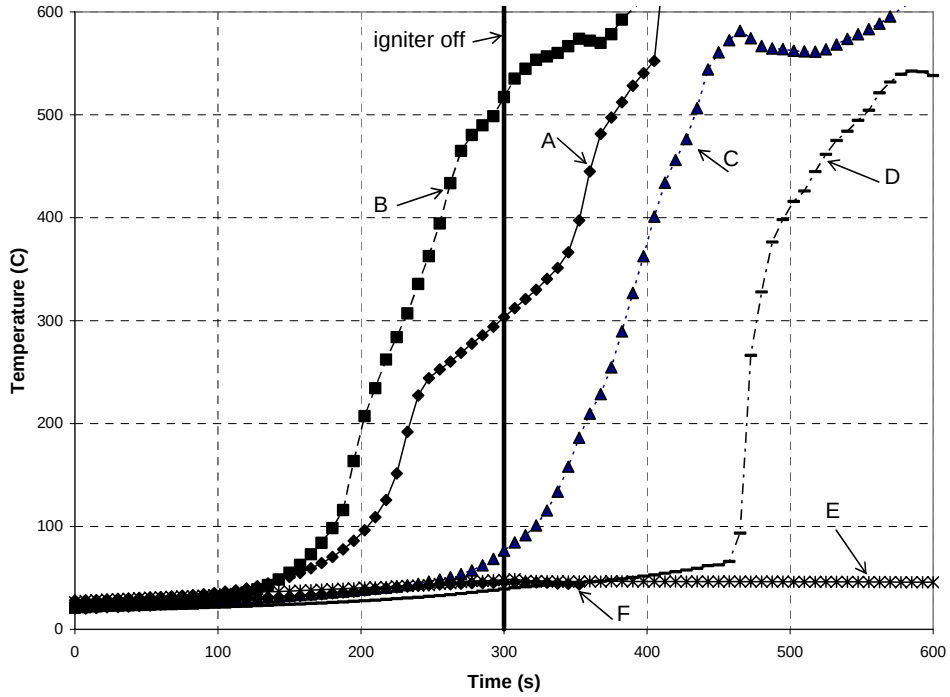

Figure 5. Belt surface temperatures at 2.44 m from the leading edge for six types of conveyor belts (A: NFR SBR 2 plies; B: NFR SBR 3 plies; C: NFR SBR 4 plies; D: FR SBR 3 plies; E: Neoprene; F: PVC)

Table 3. Temperatures (ºC) at 2.44 m from the leading edge of the belt for six types of conveyor belts

NFR SBR (2 plies)	NFR SBR (3 plies)	NFR SBR (4 plies)	FR SBR (3 plies)	FR Neoprene	FR (PVC)
302	515	77	39	48	46

Influence of Stoichiometry on Flame Spread Rates

In well-ventilated systems, such as either the large- or small-scale tunnels, there is sufficient air to generally assume that combustion occurs on the fuel-lean side of stoichiometry. However, the argument here is that the interaction of the flame with the tunnel geometry, such as contact with the roof, limits the flame surface area available for entrainment of sufficient air for combustion to occur on the fuel-lean side of stoichiometric so that the actual combustion taking place within the flame zone makes a transition to fuel-rich combustion. Standard measures of the mass generation of fuel and the mass of air available do not suffice for this determination. However, the resultant levels of CO and CO_2 produced by the flame are sensitive to the stoichiometry of the combustion process, and it was decided to measure the ratio, CO/CO_2, produced by the propagating flames and to relate this ratio to the equivalence ratio, φ. For the SBR samples, previous data [14] indicated that the yields of CO and CO_2 under oxygen-rich conditions had the respective values of $Y_{CO} = 0.072$ g/g and $Y_{CO2} = 1.91$ g/g. Furthermore, the decrease in the yield of CO_2 and the increase in the yield of CO as a function of the equivalence ratio, φ, could be put in the forms given by Tewarson [15], namely,

$$Y_{CO2} = 1.91[1 - \exp(-2.5\varphi^{-1.2})] \quad (1)$$

$$Y_{CO} = 0.072[1 + 2.5\exp(-2.5\varphi^{-2.8})] \quad (2)$$

Using these two expressions, the CO/CO2 concentration ratio becomes

$$CO/CO_2 = 1.576(Y_{CO}/Y_{CO2}) \quad (3)$$

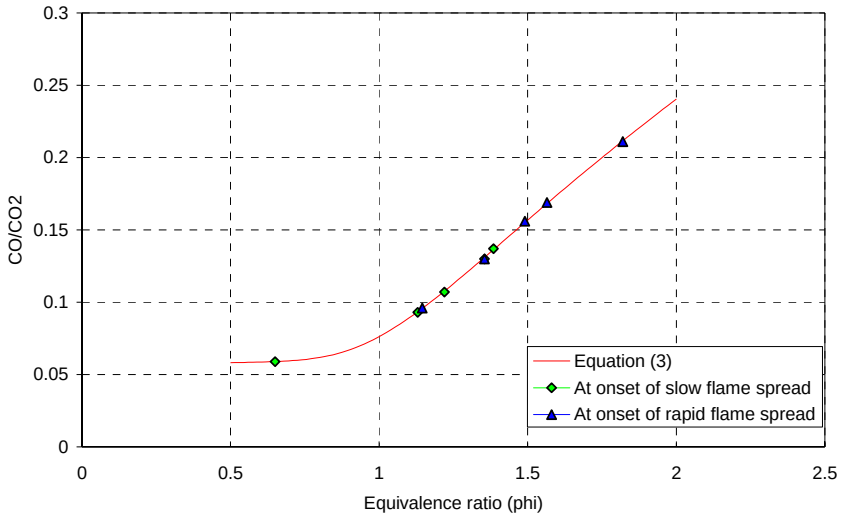

Figure 6. The gas concentration ratio, CO/CO2, vs. the equivalence ratio, φ, for samples of SBR using the formulation of Tewarson [15]

Figure 6 is a plot of this ratio as a function of the equivalence ratio, φ. The symbols on the curve represent values of the ratio measured experimentally in the fire gallery tests [4] during the early stages of low flame spread rates and just prior to the onset of much more rapid flame spread. In general, these tests

yielded the same trends in terms of flame spread pattern. It was observed that, after flames had been established on the surface of the sample in the ignition area, the flame front advanced rather slowly along the surface of the sample until approximately 40% of the sample surface was involved. At this point, a period of rapid flame spread occurred where flames propagated to the end of the sample in 60 to 90 seconds.

Figure 7 shows the measured CO/CO_2 ratios obtained at different air velocities and for different surface-to-roof distances, H, between the sample surface and the roof of the tunnel. Also shown in Fig. 6 are the measured CO/CO2 ratios from the large-scale tests [4]. At H = 0.22 m in the small-scale tunnel, the CO/CO_2 ratio has a fuel-rich value only at the lowest air velocity of 0.7 m/s because the fuel-rich occurs when the CO/CO_2 ratio is great than 0.08 as shown in Figure 5. For greater air velocities, this ratio has an average value of 0.068 ($\varphi = 0.90$), in reasonable agreement with the over-ventilated ratio of 0.060. For H = 0.11 m, the CO/CO_2 ratios are indicative of fuel rich combustion with the measured flame front velocities having a maximum value (0.97 cm/s) at a convective air velocity of about 2.2 m/s. In addition, at the highest convective air velocity, (3.2 m/s), both the flame front velocity and the CO/CO_2 ratio show significant decreases.

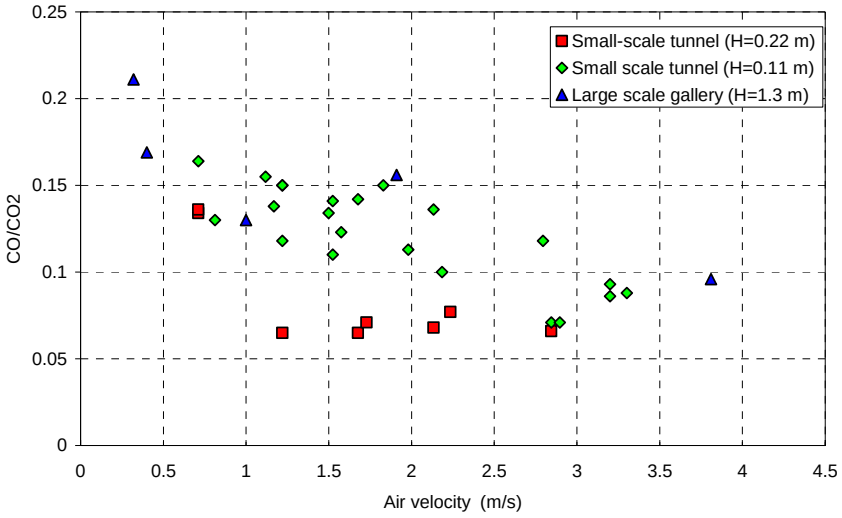

Figure 7. Measured CO/CO_2 concentration ratios in the small-scale experiments as a function of the forced convective velocity for surface-to-roof distances of 0.11 and 0.22 m

The data show that at low air velocities, or, alternatively, small separations between the roof and the surface of the combustible, the combustion usually occurs in the fuel-rich region, and that within this region, more rapid flame spread rates are observed. The conclusion is that under these conditions, the geometry of the system in which flame spread occurs limits the accessibility of oxygen to the flame. This is different from the flame spread in an open space in which oxygen can be entrained by the flame from all directions. As discussed before, the flame spread rate in an open space increases with the forced convective airflow. For the flame spread in a confined space, this relationship is generally not valid and other factors must be considered. One of these, as discussed above is the increased radiative flux. Modeling this transition in the simple manner discussed above [11], does indeed result in increases in the radiative flux and higher flame front velocities, but in addition, there may also exist changes in the radiative properties of soot formed in the fuel-rich region. Tewarson [15] found that as the φ increases, the yield of hydrocarbons increases dramatically and at rates that may be a factor of 10 greater than the increase in CO yields. It appears reasonable, then, that the soot formed under fuel-rich combustion conditions may also contain a larger fraction of hydrocarbons, and that this increase in the volatile fraction of the soot can alter the radiative properties of the flame. Scherrer et al [16] measured the specific absorption, σ_{ABS} (m^2/g), (at $\lambda = 550$ nm) of soot produced at the exhaust of a diesel engine at volatile fractions, γ, ranging from 0.052 to 0.578. From this data, it is found that σ_{ABS} varies with γ and λ via the

expression

$$\sigma_{ABS} = (5.0/\lambda)(1 - \gamma) \quad (4)$$

In general, the mean absorption coefficient for soot, κ_S, used to characterize flame soot radiation is given by [17]

$$\kappa_S = 258.55 C_0 f_V T_F \quad (5)$$

where f_V is the soot volume fraction (m^3/m^3), T_F is the flame temperature (K), and C_0 represents some average optical constant for the soot, with a typical value of 4.6. Since C_0 corresponds to the factor $5.0/(1- \gamma)$ appearing in equation (4), it can be inferred that typical flame soot radiation is calculated at a volatile fraction, γ, equal to about 0.08, a value typical of over-ventilated combustion. Now, f_V varies approximately linearly with soot yield, Y_S, and for constant T_F, equation (5) would predict that, as Y_S increases (due to increases in φ), κ_S also increases. However, if C_0 decreases as γ increases and γ increases as φ increases, then the value of κ_S would depend upon the relative increases of both γ and Y_S as a function of φ. While soot yields as a function of φ have been measured for a number of combustible polymers, any corresponding relationships between γ and φ have received little attention. Since flame soot is the primary source of flame radiation and in view of the results obtained above, indicating that flame spread typically occurs for $\varphi > 1$, and since fuel-rich combustion can result in dramatic increases in flame front velocities, it would appear that the effects of φ on γ and the resultant impact on the optical and radiative properties of soot warrant further investigation and quantification. Utilization of some average set of soot optical properties, independent of stoichiometry, may suffice when combustion occurs in over-ventilated systems, but may be grossly inadequate to describe the radiative properties of fuel-rich combustion.

CONCLUSIONS

The experimental results of this study indicate that the flammability of various conveyor belts is greatly dependent on the test method. With a sufficient igniter heat output, 21 kW, a ventilation velocity of 1.02 m/s and the belt surface-to-roof distance of 0.22 m in this study, all FR and NFR belts could be ignited and the flame propagated to the end of the belts in the small-scale tunnel. The FR conveyor belts have lower values of heat of combustion resulting in smaller flame spread rates compared with the NFR belts. PVC belt only burned on the surfaces. The ventilation velocity and the belt surface-to-roof distance were found to affect each other. With the ventilation velocity greater than 1.52 m/s, the FR SBR belt could not propagate flame at a belt surface-to-roof distance of 0.22 m, while the flame spread on the belt occurred at the belt surface-to-roof distance of 0.11 m. Flame spread typically occurred for $\varphi > 1$, and that fuel-rich combustion could result in dramatic increases in flame front velocities.

ACKNOWLEDGEMENTS

The authors wish to acknowledge the assistance from Richard A. Thomas and Kenneth E. Mura in conducting the conveyor belt tests.

REFERENCES

1. DeRosa, M., 2004. Analysis of mine fires for all U.S. underground and surface coal mining categories, 1990-1999. *NIOSH Information Circular*, 9470.
2. U.S. Code of Federal Regulations, 2001. Title 30, Part 75.
3. Lazzara, C.P. and Perzak, F.J., 1989. Conveyor belt flammability tests: Comparison of large-scale gallery and laboratory-scale tunnel results. *23rd International Conference of Safety in Mines Research Institutes*, Washington, DC, pp. 138-150.
4. Lazzara, C.P. and Perzak, F.J., 1987. Effect of ventilation on conveyor belt fires. *Proceedings of Symposium on Safety in Coal Mining*, Pretoria, South Africa.
5. Verakis, H.C. and Dalzell, R.W., 1988. Impact of entry air velocity on the fires hazards of conveyor belts. *Fourth International Mine Ventilation Congress*, Brisbane, Australia, pp. 375-

381.
6. MSHA, 1989. Fire testing procedures and construction drawings for the belt evaluation laboratory test, MSHA Approval and Certification Center.
7. Verakis, H.C., 1991. Reducing the Fire Hazard of Mine Conveyor Belts. *Proceedings of the 5th US Mine Ventilation Symposium*, Society for Mining, Metallurgy, and Exploration, Inc. (SME), Littleton, CO, pp. 69-73.
8. Perzak, F.J. and Lazzara, C.P., 1992. Flame spread over horizontal surfaces of polymethylmethacrylate. *Twenty-fourth Symposium (International) on Combustion*, The Combustion Institute, Pittsburgh, PA, pp. 1661-1668.
9. Fernandez-Pello, A.C. and Hirano, T., 1983. Controlling Mechanisma of Flame Spread. *Combustion Science and Technology*, 32, 1-31.
10. Fernandez-Pello, A.C., 1984. Flame spread modelling. *Combustion Science and Technology*, 39, 119-134.
11. Hwang, C. C., Litton, C. D., Perzak, F. J. and Lazzara, C. P., 1991. Modeling the flow-assisted flame spread along conveyor belt surfaces. *Proceedings of the 5th U. S. Mine Ventilation Symposium*, Society for Mining, Metallurgy, and Exploration, Inc. (SME), Littleton, CO, pp. 39-44.
12. Litton, C.D., Mura,, K.E., Thomas, R.A. and Veraski, H.C., 2003. Flammability studies of noise abatement materials used in cabs of large mobile mining equipment. *Proceeding of Fire and Materials 2003 International Conference*, San Francisco, CA.
13. Egan, M., 1988. Combustion Products from Burning Conveyor Belts. *US Bureau of Mines IC*, 9205.
14. Tewarson, A., Jiang, F. H., and Morikawa, T., 1993. Ventilation-controlled combustion of polymers. *Combustion and Flame*, 95, 151-169.
15. Scherrer, H. C., Kittelson, D. B., and Dolan, D. F., 1982. Light Absorption Measurements of Diesel Particulate Matter. *SAE Paper 810181*, Society of Automotive Engineers.
16. Tien, C. L., Lee, K. Y., and Stretton, A. J., 1988. Radiation Heat Transfer. *SFPE Handbook of Fire Protection Engineering*, Chap. 1-5, pp 1-92-1-106.